

Ramakanth Pagadala,^{a,*} Nilesh V. Gandhare,^a Uppalaiah Kusampally,^b Venkateshwarlu Jetti,^a Jyotsna S. Meshram,^{a,*} and H. D. Juneja^a

^aDepartment of Chemistry, Rashtrasant Tukadoji Maharaj Nagpur University, Nagpur 440 033, Maharashtra, India

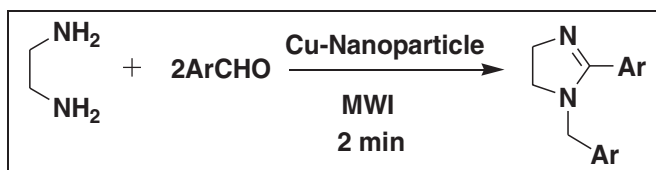
^bDepartment of Chemistry, Osmania University, Hyderabad 500 007, Andhrapradesh, India

*E-mail: pagadalaramakanth@gmail.com or drjmeshram@rediffmail.com

Received September 15, 2011

DOI 10.1002/jhet.1551

Published online 10 October 2013 in Wiley Online Library (wileyonlinelibrary.com).



Series of 1-arylmethyl-4,5-dihydro-2-aryl-1*H*-imidazole were synthesized expeditiously in good yields from 1,2-diaminoethane and aromatic aldehydes in the presence of Cu nanoparticle under microwave irradiation in solvent-free method. Monodisperse spherical Cu nanoparticles with a diameter range of 45 ± 8 nm were synthesized by polyol process. The particle size and elemental structure of copper nanoparticles were confirmed by XRD data and was found to be having a face-centered cubic structure. The resulting substituted imidazoles have been studied in the achievement of degree of drug absorption enhancement as well as the potential associated toxicity on the basis of hypothetical antibacterial pharmacophores and structures that were designed to interact with both of gram-positive and gram-negative bacteria. All the synthesized molecules were characterized on the basis of ¹H NMR, ¹³C NMR, mass spectrometry, and elemental data.

J. Heterocyclic Chem., **51**, 116 (2014).

INTRODUCTION

The pharmaceutical industry invests great sums of money in the development of drugs that can be effective in application to pathologies that affect major population groups or in treating new diseases. In this challenging task and apart from the pharmacological effects that represent the first development step, it is of great relevance to consider the biopharmaceutical and pharmacokinetic properties of the drug, particularly those concerning intestinal absorption and bioavailability (BA). Hence, in this article, we have employed to achieve simple and environmentally compatible synthetic methodology for the synthesis of substituted 1*H*-imidazoles in the presence of Cu nanoparticle/zeolite under microwave (MW) irradiation.

Substituted imidazoles are synthetically important because of their use as a synthetic intermediates [1], catalysts [2], chiral auxiliaries [3], chiral catalysts [4,5], and ligands for asymmetric catalysis [6,7] in various synthetic reactions. There are several synthetic methods for 2-imidazolines starting mainly from aldehydes and ethylenediamine with NBS [8]. Recently, the organic reactions under MW irradiation have attracted attention of scientists because of their high reaction rate, mild reaction conditions, and the formation of clean products [9,10]. MW irradiations have attracted considerable attention in the past decade for the efficient and relatively friendlier synthesis of a variety of inorganic and organic compounds [11]. Over the past several years, chemists have been aware of the environmental implications of their

chemistry. Nowadays, they are trying to develop new synthetic methods, reaction conditions, and uses of chemicals that reduce risks to humans and the environment. Organic solvents are high on the list of damaging chemicals because they are employed in huge amounts and are usually volatile liquids that are difficult to store.

Microwave-assisted synthesis is generally much faster, cleaner, and more economical than the conventional methods [12]. Rate enhancements when using MW energy have been reported for a number of organic synthesis as well as Cu nanoparticle catalyzes various organic reaction [13,14]. In the present study, we have synthesized nanocopper that was reported in literature [15], in which highly monodisperse copper nanoparticles in ambient atmosphere synthesized. Diethylene glycol (DEG) in nonaqueous solvent as a reaction medium allows us to minimize the copper surface oxidation. Furthermore, poly(vinylpyrrolidone) was added as a dispersing agent also effectively prevents the oxidation process. In the case of Cu-nanoparticle synthesis, the reducing ability of DEG is insufficient to reduce the copper ions because copper is easily oxidized to either CuO or Cu₂O in air atmosphere. Here, NaH₂·PO₂·H₂O used as reducing agent for the preparation of Cu nanoparticles.

Nowadays, the researchers are much interested on theoretical molecular property [16] to explain the bacteria inhibition of heterocycles. Our main interesting tasks of this effort were to investigate the utility of robust prediction models for the heterocycles/bacteria inhibitory properties (solubility, BA, drug likeness, toxicity study, etc.) of small

molecules using Molinspiration. Osiris model values were compared with experimental antibacterial results for the design of specific new compounds that were found to be correlation. Previously, we reported the synthesis of 1*H*-imidazoles in the presence of zeolite [17]. We now report a new synthetic approach to demonstrate the excellent catalytic activity of Cu nanoparticles for the synthesis of substituted 1*H*-imidazoles under MW irradiation.

RESULTS AND DISCUSSION

Chemistry. We have selected from literature only one synthesis condition for preparation of copper particles as follows. Poly(*N*-vinylpyrrolidone) (PVP, $M_w = 40,000$), acting as a capping molecule, was dissolved in DEG (99%). Sodium phosphinate monohydrate ($\text{NaH}_2\text{PO}_2 \cdot \text{H}_2\text{O}$) 17.53 mmol, used as a reducing agent, was added to the DEG solution, and the solution was heated to reaction temperatures (140°C). The aqueous solution of copper(II) sulfate pentahydrate 20 mmol was then injected into the hot reaction medium via a syringe pump. The injection rate of the Cu salt solution was 8 mL/min. The particles synthesized in ambient atmosphere were determined to be phase-pure Cu without any impurity phase. X-ray diffraction patterns correspond to crystalline copper characteristic peaks with a face-centered-cube crystal structure as shown in Figure 1.

Earlier, we have synthesized substituted imidazoles [17] (Scheme 1). In the present study, synthesis of 1*H*-imidazoles was carried out by mixing 1,2-diaminoethane with different substituted aromatic aldehydes in the presence of Cu nanoparticles under MW irradiation as well as classical method (Scheme 2). In MW method, the yield of the entire

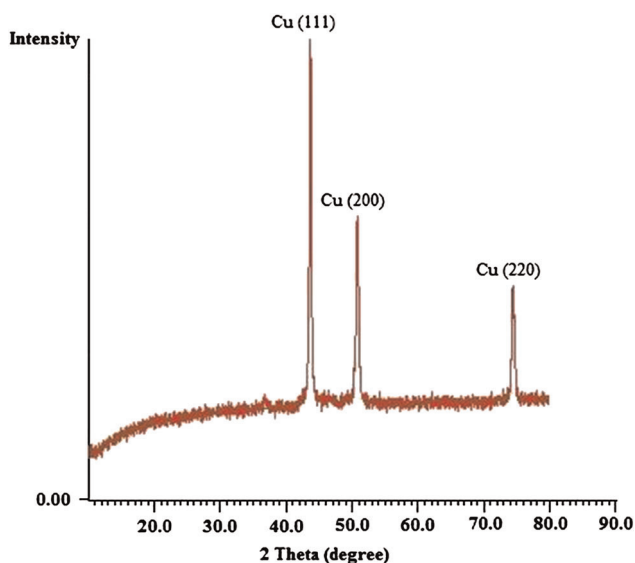
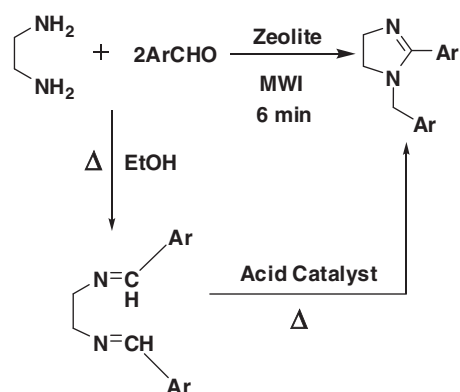


Figure 1. X-ray diffraction pattern of Cu nanoparticles. [Color figure can be viewed in the online issue, which is available at wileyonlinelibrary.com.]

Scheme 1. Synthesis of substituted imidazoles [17].



1*H*-imidazoles is more than the classical method. All the 1-arylmethyl-4, 5-dihydro-2-aryl-1*H*-imidazoles derivatives were obtained in excellent yields. The values as yield and reaction time for both the method are showed in Table 1. The efficiency of MW-assisted method and the classical method becomes clearer as shown in Figure 2. Physical properties of the substituted imidazoles are given in Table 2. Additionally, there are distinct advantages of these solvent-free protocols because they provide reduction or elimination of solvents thereby preventing pollution in organic synthesis “at source”.

Biological activity: Antibacterial studies. In Table 3, it was observed that all the tested compounds possess moderate to good inhibition. Potency against different bacterial strain compounds **3**, **5**, and **7** against *Bacillus megaterium*, compound **7** for *Bacillus subtilis*, compound **1** for *Escherichia coli*, compounds **1**, **3**, **5**, and **7** for *Klebsiella pneumoniae*, compounds **3** and **5** for *Proteus vulgaris*, and compound **7** for *Staphylococcus aureus* has shown very good activity that was found to be almost equivalent to that of standard.

Whereas, the compounds **1** and **4** for *B. megaterium*, compounds **2**, **4**, and **5** for *B. subtilis*, compounds **3**, **4**, **6**, and **7** for *E. coli*, compounds **2** and **6** for *K. pneumoniae*, compounds **1**, **4**, and **7** for *P. vulgaris*, and compounds **1**, **2**, **5**, and **6** for *S. aureus* have shown moderate activity.

Molinspiration calculations [18,19]. We calculate the MiLogP (octanol/water partition coefficient) by the methodology developed by Molinspiration as a sum of fragment-based contributions and correction factors (Tables 4 and 5). The molecular polar surface area (TPSA) is also calculated based on the methodology published by Ertl et al. as a sum of fragment contributions [20] in which O-centered and N-centered polar fragments are considered. Polar surface area (PSA) shows very good descriptor characters of drug absorption including intestinal absorption, BA, Caco-2 permeability and blood–brain barrier penetration. The predicted

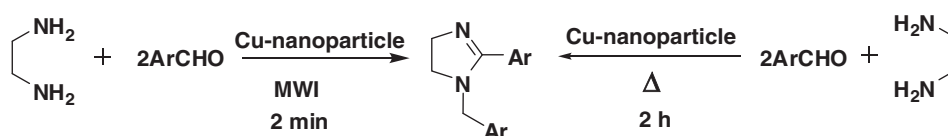
Scheme 2. Microwave-assisted synthesis of 1*H*-imidazoles in the presence of Cu nanoparticles.

Table 1

Time and yield comparison between classical and microwave irradiation.

Compound	Formula weight	Microwave method Cu nanoparticle (zeolite)		Classical method Cu nanoparticle (without catalyst)	
		Reaction time (min)	Yield (%) ^a	Reaction time (h)	Yield (%) ^a
1	268	2	94 (91)	2	76 (65)
2	326	2	93 (90)	2.5	75 (61)
3	356	2	91 (85)	2.3	77 (58)
4	322	2	95 (92)	2	79 (61)
5	272	2	92 (86)	2.1	72 (56)
6	326	2	91 (82)	2	80 (60)
7	216	2	90 (80)	2	78 (59)

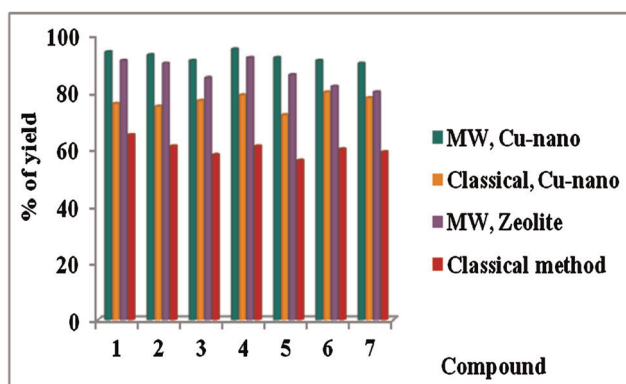
^aIsolated yields.

Figure 2. Graphical representation of yield comparison between classical and microwave (MW) irradiation. [Color figure can be viewed in the online issue, which is available at wileyonlinelibrary.com.]

molecular property results of compounds 1–7 (MiLogP, TPSA, GPCR ligand, and ICM) are depicted in Tables 4 and 5 using mol inspiration software programs and

compared them with the values obtained for reference drug Ampicillin. LogP value (Lipophilicity) and PSA values are two important properties for the prediction of per oral BA of drug molecules [21]. For all the compounds, the calculated logP values are below 5, which is the upper limit for the drugs to be able to penetrate through biomembranes according to Lipinski's rules. These low logP values are indicating the lowest degree of lipophilicity; thus, it is an indication for good water solubility of all the compounds 1–7.

The PSA is evaluated from the surface areas that are occupied by oxygen and nitrogen atoms and by hydrogen atoms attached to them. Thus, the PSA is closely related to the potential of hydrogen bonding of a compound [21]. Molecules with PSA values of 140 Å² or more are estimated to illustrate poor intestinal absorption [21]. Table 4 shows that all the compounds that are much below the limit (140 Å²) are having well intestinal absorption. It should be remembered that logP and PSA values play important role, although some other criteria is needed to study the oral

Table 2

Physical and analytical data of substituted imidazoles.

Compound	Ar	Formula	mp (°C)	% Calcd (found)		
				C	H	N
1	<i>o</i> -OHC ₆ H ₄	C ₁₆ H ₁₆ N ₂ O ₂	90	71.62 (71.65)	6.01 (6.04)	10.44 (10.46)
2	<i>m</i> -NO ₂ C ₆ H ₄	C ₁₆ H ₁₄ N ₄ O ₄	119	58.89 (58.86)	4.32 (4.35)	17.17 (17.20)
3	<i>m, p</i> -(OCH ₃) ₂ C ₆ H ₄	C ₂₀ H ₂₄ N ₂ O ₄	115	67.40 (67.47)	6.79 (6.82)	7.86 (7.84)
4	<i>p</i> -(CH ₃) ₂ NC ₆ H ₄	C ₂₀ H ₂₆ N ₄	127	74.50 (74.53)	8.13 (8.15)	17.38 (17.39)
5	<i>p</i> -FC ₆ H ₄	C ₁₆ H ₁₄ N ₂ F ₂	97	70.58 (70.59)	5.18 (5.16)	13.95 (13.98)
6	<i>o</i> -NO ₂ C ₆ H ₄	C ₁₆ H ₁₄ N ₄ O ₄	104	58.89 (58.92)	4.32 (4.34)	17.17 (17.20)
7	2-furyl	C ₁₂ H ₁₂ N ₂ O ₂	121	66.65 (66.60)	5.59 (5.64)	12.96 (12.98)

Table 3

Antibacterial activity of imidazoles (zone of inhibition in mm).

Compound	Bacteria (MIC at 100 µg/mL)					
	Gram (+) bacteria				Gram (-) bacteria	
	A	B	C	D	E	F
1	++	+	++	++	+++	+++
2	+	++	++	+	++	-
3	+++	-	+	+++	+++	++
4	++	++	-	++	+	++
5	+++	++	++	+++	+++	+
6	+	-	++	-	++	++
7	+++	+++	+++	++	+++	++
control	-	-	-	-	-	-
Ampicillin	+++	+++	+++	+++	+++	++

MIC, minimum inhibitory concentration.

Key to symbols: A, *Bacillus megaterium*; B, *Bacillus subtilis*; C, *Staphylococcus aureus*; D, *Proteus vulgaris*; E, *Klebsiella pneumoniae*; F, *Escherichia coli*.

Inactive = - (inhibition zone <5 mm); slightly active = + (inhibition zone 5–12 mm); moderately active = ++ (inhibition zone 13–17 mm); highly active = +++ (inhibition zone >17 mm).

absorption of a drug in human body. To strengthen this contention, note that all the compounds have zero N-violations of the Lipinski's rules. Two or more violations of this rule suggest that the probability of problems in BA [22] for all the compounds (**1–7**); therefore, there is no problem in BA.

The properties, mainly hydrophobicity, electronic distribution, hydrogen bonding characteristics, molecule size and flexibility, and presence of various pharmacophores features, influence the behavior of molecule in a living organism, including BA, transport properties, affinity to proteins, reactivity, toxicity, metabolic stability, and many others. Because of the activity/nature of these properties, drug likeness may be defined as a complex balance of various molecular properties and structure features that determine whether particular molecule is similar to the known drugs. Activity of all seven compounds and standard drug was strictly analyzed under four criteria of known successful drug activity in the areas of G-protein

Table 5Drug likeness of compounds (**1–7**).

Compound	GPCR	ICM	KI	NRL
1	0.05	-0.16	-0.38	-0.52
2	-0.08	-0.24	-0.53	-0.61
3	0.08	-0.16	-0.36	-0.46
4	0.12	-0.13	-0.36	-0.46
5	0.19	-0.06	-0.38	-0.58
6	-0.14	-0.29	-0.50	-0.54
7	-0.32	-0.64	-0.83	-2.29
AMP	-0.56	-0.43	-0.90	-0.10

coupled receptors (GPCR) ligand activity, ion channel modulation, kinase inhibition activity, and nuclear receptor ligand activity. Thus, it was found that all compounds having consistent negative values were compared with the value of standard drug used. Drug likeness of compounds **1–7** is tabulated in Table 5. The values of all the compounds are below the value of standard drug. Therefore, it is an indication for good activity of compounds **1–7** compared with reference drug used on the basis of these four rigorous criteria, that is, GPCR ligand, ion channel modulator, kinase inhibitor, and nuclear receptor ligand.

Osiris calculations [18,23]. The data base of CELERON Company of Swiss was used to classify the remarkably well-behaved mutagenicity of diverse synthetic molecules and to quantify the role played by various organic groups in promoting or interfering with the way a drug can associate with DNA. The cytochromes P450 are the one very important class of enzymes, responsible for many ADMET problems. Inhibition of these or production of unwanted metabolites can result in many adverse drug reactions. Toxicity risks (mutagenicity, tumorigenicity, irritation, and reproduction) and physicochemical properties [miLogP, solubility, drug likeness, and drug score (DS)] of compounds **1–7** evaluated by the methodology developed by Osiris are tabulated in Table 6. The toxicity risk predictor locates groups within a molecule, which shows a potential toxicity risk. Toxicity risk alerts are an indication that the drawn structure may be harmful concerning the risk

Table 4Molinspiration calculations of compounds (**1–7**).

Compound	MW	miLogP	TPSA	OH-NH	NViol	Vol
1	268	2.329	56.058	2	0	247.096
2	326	2.318	107.25	0	0	277.728
3	356	1.741	52.538	0	0	333.243
4	322	2.652	22.078	0	0	322.872
5	272	2.775	15.602	0	0	240.923
6	326	2.27	107.25	0	0	277.728
7	216	0.962	41.882	0	0	194.196
AMP	349	-0.87	113	4	0	299

Table 6
Osiris calculations of compounds (1–7).

Compound	Prediction of toxicity risks				Molecular properties' calculations				
	MUT	TUMO	IRRI	REP	MW	CLP	LogS	DL	D-S
1	–	–	–	–	268	2.23	–2.19	3.47	0.9
2	Medium risk	–	–	Medium risk	326	2.56	–3.7	–1.7	0.3
3	–	–	–	–	356	2.4	–2.86	5.45	0.84
4	–	High risk	–	–	322	2.82	–2.86	3.03	0.5
5	–	–	–	–	272	2.94	–3.41	3.56	0.83
6	Medium risk	–	–	–	326	2.56	–3.7	–3.72	0.33
7	–	–	–	–	216	1.03	–2.15	3.63	0.94
AMP	–	–	–	–	349	–0.04	–1.57	10.72	0.91

category specified. The data evaluated in Table 6 indicate that most of the compounds are nonmutagenic, nonirritating with no reproductive effects when run through the mutagenicity assessment system comparable with reference drug used. The logP value of compounds is the logarithm of its partition coefficient between n-octanol and water, a well-established measure of the compound's hydrophilicity. Therefore, low hydrophilicities or high logP values that are greater than 5.0 may cause poor absorption or permeation. On this basis, all the compounds 1–7 that are having low logP values indicate well absorption. Along with this, all the compounds 1–7 have shown good antibacterial screening results compared with standard drug used because of low logP values. The aqueous solubility of a compound significantly affects its absorption and distribution characteristics in human body. Typically, a low solubility goes along with a bad absorption, and therefore, the general aim is to avoid poorly soluble compounds. Our estimated logS value is a unit stripped logarithm (base 10) of a compound's solubility measured in mol/liter. There are more than 80% of the drugs on the market have a (estimated) logS value greater than –4. The compounds are tabulated (1–7) having logS values between –2 and –4. It indicates that all the compounds show remarkable solubility goes towards well absorption. Further, Table 6 shows the drug likeness of compounds 1–7 in the comparable zone with that of reference drug used for comparison.

We have calculated overall DS for the compounds 1–7 and compared with that of reference drug Ampicillin used as shown in Table 6. The DS combines drug likeness, MiLogP, logS, molecular weight, and toxicity risks in one handy value than may be used to judge the compound's overall potential to qualify for a drug. This value is calculated/estimated by multiplying contributions of the individual properties with this equation:

$$DS = \Pi \left(\frac{1}{2} + \frac{1}{2} S_i \right) \Pi t_i$$

where $S = 1/1 + e^{ap} + b$

DS is the drug score. S_i is the contribution calculated directly from miLogP; the logS, molecular weight, and

drug likeness (pi) describe a spline curve. Parameters a and b are (1, –5), (1, 5), (0.012, –6), and (1, 0) for miLogP, logS, molecular weight, and drug likeness, respectively. t_i is the contributions taken from the four toxicity risk types. The t_i values are 1.0, 0.8, and 0.6 for no risk, medium risk, and high risk, respectively. The compounds 1–7 showed moderate to good DS as compared with standard drugs used.

Antibacterial activities of all the compounds were tested against gram-positive bacteria (*B. subtilis* and *S. aureus*) and gram-negative bacteria (*E. coli* and *K. pneumoniae*) by measuring the zone of inhibition on agar plates [14]. The compounds possess moderate to good activity against all strains in comparison with standard drug (Table 2).

CONCLUSIONS

A highly efficient MW-assisted rapid synthesis of 1*H*-imidazoles has been developed in the presence of Cu nanoparticle; all these performed reactions exhibit higher yields than that of MW-assisted synthesis of 1*H*-imidazoles in the presence of zeolite as well as usual classical reactions and have been achieved within time span of 2 min. This solvent-free neat reaction is not only of interest from an ecological viewpoint but also offers considerable certain gram-positive and gram-negative bacteria. Most of the compounds among 1–7 were found to be equally potent comparable with Ampicillin. Thus, from the data obtained from virtual and practical screening, it is concluded that the compounds were varied to possess a broad range of lipophilic character revealed by logP values. All the compounds were determined to express zero violation to the Lipinski's rules, hence an indication of much favorable BA based on drug likeness. The considerable number of hydrogen donor/acceptor atoms incurred significant hydrophilic character into the majority of these drugs (supported by logP values less than 5). Comparing relative activity scores of Ampicillin utilizing four drug classes (GPCR ligand, ion channel modulator, kinase inhibitor, and nuclear receptor ligand) showed all

compounds are very highly correlated with expected similar bioactivity. Consequently, imidazoles represent a class that needs further investigation with the hope of finding new antimicrobial agents.

EXPERIMENTAL

Chemistry. The entire chemicals and solvents Analytical Reagent (AR) grade were used without further purification. Melting points were taken in an open capillary tube. The MW-assisted synthesis of titled compounds was carried out in a CEM – 908010 (Smith Farm Rd, Mathews, N.C-28105, US), bench mate model, 300 watts laboratory MW reactor. Elemental analyses were carried out using a Perkin-Elmer (Maryland, US), CHN elemental analyzer model 2400. ¹H NMR and ¹³C NMR spectra of the imidazoles were recorded on a Bruker-Avance (300 MHz) (Switzerland), Varian-Gemini (200 MHz) spectro-photometer using DMSO solvent and TMS as the internal standard. EIMS spectra were determined on an LCQ ion trap mass spectrometer (Thermo Fisher, San Jose, CA, USA), equipped with an EI source.

Biological screening. Antimicrobial activity of all synthesized compounds was determined by agar diffusion method [24]. All human pathogenic bacteria viz. *B. megaterium*, *B. subtilis*, *E. coli*, *K. pneumoniae*, *P. vulgaris*, and *S. aureus* were obtained from the Osmania University, Hyderabad, India. Stock solutions of compounds were diluted in dimethyl sulfoxide (DMSO). Minimum inhibitory concentration was defined as the lowest concentration of compound required for a complete inhibition of the bacterial growth after incubation time. For antibacterial activity, Muller Hinton agar was used. The wells of 6-mm diameter were filled with 0.1 mL of each compound dilution separately for each test of bacterial strain. The DMSO alone was used as a control. The antibiotic Ampicillin was used as reference antibacterial for comparison. Inoculated plates were then incubated at 37°C for antibacterial activity for 24 h. After incubation, the antimicrobial activity was measured in terms of the zone of inhibition in millimeter as shown in Table 3.

Synthesis of 1-arylmethyl-4, 5-dihydro-2-aryl-1*H*-imidazoles under MW irradiation in the presence of Cu nanoparticles. 1,2-Diaminoethane (0.108 g, 1 mmol), benzaldehyde (0.212 g, 2 mmol), and Cu nanoparticles (0.03 g) were thoroughly mixed. The reaction mixture was irradiated for 2 min with 100 W microwaves at 110°C in microwave oven in the temperature control mode. The completion of the reaction was monitored by TLC. After the irradiation was over, the reaction mixture was cooled and added into water and extracted with diethyl ether. After filtering the Cu nanoparticles, the ethereal layer was washed with water, dried with anhydrous sodium sulfate, and the solvent removed. The crude product was recrystallized from methanol.

Synthesis of 1-arylmethyl-4, 5-dihydro-2-aryl-1*H*-imidazoles by classical method in the presence of Cu nanoparticles. A mixture of 1,2-diaminoethane (0.108 g, 1 mmol), benzaldehyde (0.212 g, 2 mmol), and Cu nanoparticles (0.03 g) was refluxed for ~2 h. The completion of the reaction was monitored by TLC. After completion of the reaction, the reaction mixture was set on one side to cool. Solid deposit was collected by the filtration. The crude product was recrystallized from methanol.

Preparation of 1-arylmethyl-4, 5-dihydro-2-aryl-1*H*-imidazoles under MW irradiation in the presence of zeolite [17]. 1,2-Diaminoethane (0.108 g, 1 mmol), benzaldehyde (0.212 g, 2 mmol), and zeolite (montmorillonite K-10) (0.1 g) were thoroughly mixed. The reaction mixture was irradiated for 6 min with 100 W microwaves at 110°C in microwave oven in the temperature control mode. The completion of the reaction was monitored by TLC. After the irradiation was over, the reaction mixture was cooled and added into water and extracted with diethyl ether. After filtering the zeolite particles, the ethereal layer was washed with water, dried with anhydrous sodium sulfate, and the solvent removed. The crude product was recrystallized from methanol.

Preparation of 1-arylmethyl-4, 5-dihydro-2-aryl-1*H*-imidazoles by classical method [17]. A mixture of Schiff base (0.7 mmol), catalytic amount of H₂SO₄, and ethanol (50 ml) was refluxed for ~4 h. The completion of the reaction was monitored by TLC. After completion of the reaction, the reaction mixture was set on one side to cool. Solid deposit was collected by the filtration. The crude product was recrystallized from methanol.

1-(2-Hydroxybenzyl)-4, 5-dihydro-2(2-hydroxyphenyl)-1*H*-imidazoles (1). ¹H NMR: δ 8.41 (s, 2H, -OH); 6.81–7.34 (m, 8H, Ar-CH); 4.0 (s, 2H, CH₂); 3.93 (t, *J* = 7.7 Hz, 2H, CH₂); 3.08 (t, *J* = 7.6 Hz, 2H, CH₂); ¹³C NMR: δ 163.0, 160.7, 154.7, 131.4, 129.5, 129.4, 128.2, 122.4, 120.6, 114.2, 111.2, 77.1, 76.5, 75.9; Mass spectra, *m/z* = 268 (M⁺, 100%).

1-(3-Nitrobenzyl)-4, 5-dihydro-2(3-nitrophenyl)-1*H*-imidazoles (2). ¹H NMR: δ 7.52–8.53 (m, 8H, Ar-CH); 4.04 (s, 2H, CH₂); 3.83 (t, *J* = 7.6 Hz, 2H, CH₂); 3.06 (t, *J* = 7.6 Hz, 2H, CH₂); ¹³C NMR: δ 162.6, 147.4, 147.5, 136.4, 133.3, 132.7, 132.3, 127.6, 122.8, 122.4, 117.8, 78.1, 77.5, 76.9; Mass spectra, *m/z* = 326 (M⁺, 100%).

1-(3, 4-Dimethoxybenzyl)-4, 5-dihydro-2(3, 4-dimethoxyphenyl)-1*H*-imidazoles (3). ¹H NMR: δ 6.41–7.1 (m, 6H, Ar-CH); 3.80 (s, 2H, CH₂); 3.61 (s, 12H, CH₃); 3.56 (t, *J* = 7.6 Hz, 2H, CH₂); 2.86 (t, *J* = 7.7 Hz, 2H, CH₂); ¹³C NMR: δ 162.5, 150.6, 148.8, 148.4, 146.8, 129.3, 125.3, 122.2, 120.5, 114.9, 114.5, 112.2, 76.4, 75.7, 74.9, 47.9; Mass spectra, *m/z* = 356 (M⁺, 100%).

1-(4-Dimethylaminobenzyl)-4, 5-dihydro-2(4-dimethylaminophenyl)-1*H*-imidazoles (4). ¹H NMR: δ 7.60 (d, *J* = 9 Hz, 2H, Ar-CH); 7.31 (d, *J* = 8 Hz, 2H, Ar-CH); 6.90 (d, *J* = 9 Hz, 2H, Ar-CH); 6.60 (d, *J* = 9 Hz, 2H, Ar-CH); 3.98 (s, 2H, CH₂); 3.72 (t, *J* = 7.6 Hz, 2H, CH₂); 3.12 (t, *J* = 7.5 Hz, 2H, CH₂); 2.98 (s, 12H, CH₃); ¹³C NMR: δ 162.7, 152.3, 132.3, 129.9, 124.9, 123.0, 112.0, 110.9, 78.1, 77.5, 76.9, 40.6; Mass spectra, *m/z* = 322 (M⁺, 100%).

1-(4-Florobenzyl)-4, 5-dihydro-2(4-florophenyl)-1*H*-imidazoles (5). ¹H NMR: δ 7.64 (d, *J* = 8 Hz, 2H, Ar-CH); 7.24 (d, *J* = 8 Hz, 2H, Ar-CH); 7.09 (d, *J* = 9 Hz, 2H, Ar-CH); 6.98 (d, *J* = 9 Hz, 2H, Ar-CH); 3.84 (s, 2H, CH₂); 3.69 (t, *J* = 7.6 Hz, 2H, CH₂); 3.01 (t, *J* = 7.6 Hz, 2H, CH₂); ¹³C NMR: δ 163.0, 160.2, 131.4, 129.5, 127.1, 125.4, 113.9, 113.4, 76.7, 75.0, 74.2; Mass spectra, *m/z* = 272 (M⁺, 100%).

1-(2-Nitrobenzyl)-4, 5-dihydro-2(2-nitrophenyl)-1*H*-imidazoles (6). ¹H NMR: δ 7.32–8.51 (m, 8H, Ar-CH); 3.82 (s, 2H, CH₂); 3.73 (t, *J* = 7.7 Hz, 2H, CH₂); 2.96 (t, *J* = 7.6 Hz, 2H, CH₂); ¹³C NMR: δ 161.6, 147.8, 147.3, 135.8, 132.4, 129.2, 127.8, 127.0, 122.1, 77.6, 76.8, 76.0; Mass spectra, *m/z* = 326 (M⁺, 100%).

1-(Furyl)-4, 5-dihydro-2(furyl)-1*H*-imidazoles (7). ¹H NMR: δ 7.86 (d, *J* = 2 Hz, 1H); 7.38d, *J* = 2 Hz, 1H); 6.22–6.69 (m, 3H); 6.24 (d, *J* = 3 Hz, 1H); 4.54 (s, 2H, CH₂); 3.45 (t, *J* = 7.5 Hz, 2H, CH₂); 2.93 (t, *J* = 7.6 Hz, 2H, CH₂); ¹³C

NMR: δ 164.3, 146.9, 143.2, 142.4, 139.6, 109.9, 109.5, 109.2, 104.6, 77.4, 76.5, 75.7; Mass spectra, $m/z=216$ (M^+ , 100%).

Acknowledgments. The authors are thankful to the head of the Chemistry Department Rashtrasant Tukadoji Maharaj Nagpur University for providing laboratory facilities. We are grateful to the Indian Institute of Chemical Technology (IICT), Hyderabad for the help in undertaking NMR and mass spectra. Special thanks are due to the Head, Department of Botany, Osmania University, Hyderabad for antimicrobial screening.

REFERENCES AND NOTES

- [1] (a) Rondu, F.; Le Bihan, G.; Wang, X.; Lamouri, A.; Touboul, E.; Dive, G.; Bellahsene, T.; Pfeiffer, B.; Renard, P.; Guardiola-Lemaître, B.; Manechez, D.; Penicaud, L.; Ktorza, A.; Godfroid, J. J. *J. Med Chem* 1997, 40, 3793.
- [2] Bousquet, P.; Feldman, J. *Drugs* 1999, 58, 799.
- [3] Ueno, M.; Imaizumi, K.; Sugita, T.; Takata, I.; Takeshita, M. *Int J Immunopharmac* 1995, 17, 597.
- [4] Hayashi, T.; Kishi, E.; Soloshonok, V. A.; Uozumi, Y. *Tetrahedron Lett* 1996, 37, 4969.
- [5] Jung, M. E.; Huang, A. *Org Lett* 2000, 2, 2659.
- [6] Corey, E. J.; Grogan, M. J. *Org Lett* 1999, 1, 157.
- [7] Isobe, T.; Fukuda, K.; Araki, Y.; Ishikawa, T. *Chem Commun* 2001, (3), 243.
- [8] Fujioka, H.; Murai, K.; Ohba, Y.; Hiramastu, A.; Kita, Y. *Tetrahedron Lett* 2005, 46, 2197.
- [9] Lidström, P.; Tierney, J.; Wathey, B.; Westman, J. *Tetrahedron* 2001, 57, 9225.
- [10] Kidwai, M.; Sapra, P.; Bhushan, K. R.; Misra, P. *Synthesis* 2001, 1509.
- [11] (a) Ramakanth P.; Parvez A.; Jyotsna S. M. *J. Coordination Chem* 2009, 62, 4009; (b) Varma, R. S. *Green Chem* 1999, 1, 43; (c) Gabriel, C.; Gabriel, S.; Grant, E. H.; Halstead, B. S. J.; Mingos, D. M. P. *Chem Soc Rev* 1998, 27, 213; (d) Kaczmarek M. T.; Renata, J.; Holderna-Kedzia, E.; Radecka-Paryzek, W. *Inorg Chim Acta* 2009, 362, 3127; (e) Dede, B.; Karićin, F.; Cengiz, M. J. *Hazardous Materials* 2009, 163, 1148; (f) Caddick, S. *Tetrahedron* 1995, 51, 10403; (g) Galema, S. A. *Chem Soc Rev* 1997, 26, 233; (h) Fini, A.; Breccia, A. *Pure Appl Chem* 1999, 71, 573.
- [12] Loupy, A.; Laurence, P.; Marion, L.; Karine, B.; Michel, M. *Pure Appl Chem* 2001, 73, 161.
- [13] Samim, M.; Kaushik, N. K.; Amarnath M. *Bull. Mater. Sci.* 2007, 30, 535.
- [14] Kidwai, M.; Bansal, V.; Saxena, A.; Aerry, S.; Mozumdar, S. *Tetrahedron Lett* 2006, 47, 8049.
- [15] Bong, K. P.; Sunho, J.; Dongjo, K.; Jooho, M.; Soonkwon, L.; Jang, S. K. *J. Colloid Interface Sci* 2007, 311, 417.
- [16] Ali, P.; Jyotsna, M.; Vandana T.; Javed, S.; Rajendra, D.; Moulay, H. Y.; Taibi, B. H. *European J. Med Chem* 2010, 45, 4370.
- [17] Ramakanth, P.; Meshram, J. S.; Himani, N. C.; Nagender, R. P. *J. Heterocyclic Chem* 2010, 47, 350.
- [18] Parvez, A.; Jyotsna, M.; Moulay, H. Y.; Taibi, B. H. *Phosphorus Sulfur Silicon Relat Elem* 2010, 185, 1500.
- [19] www.Molinspiration.com
- [20] Ertl, P.; Rohde, B.; Selzer, P. *J Med Chem* 2000, 43, 3714.
- [21] Clark, D. E.; *J Pharm Sci* 1999, 88, 807.
- [22] Lipinski, C. A.; Lombardo, F.; Dominy, B. W.; Feeney, P. J. *Adv Drug Deliv Rev* 2001, 46, 3.
- [23] www.osiris.com
- [24] Fairbrother, R. W.; Martyn, G. J. *Clin Pathol* 1951, 4, 374.